Supporting Information

Wen et al. 10.1073/pnas.0910302107

SI Materials and Methods

Reagents and Animals. The NRG1 used is a recombinant polypeptide containing the entire EGF domain of the β-type NRG1 (rHRG β177–244) (1). Ecto-ErbB4 was prepared as previously described (2). DL-2-amino-5-phosphonovaleric acid (DL-AP5), 6-cyano-7-nitroquinoxaline-2,3-dione (CNQX), and bicuculline were purchased from Tocris Bioscience; Oregon Green 488 biocytin was from Invitrogen; and diazepam was from Hospira. Other chemicals were from Sigma-Aldrich. For chemicals that had to be dissolved in dimethyl sulfoxide (DMSO), the final concentration of DMSO was ≤ 0.01% when applied to brain slices.

Rabbit polyclonal anti-ErbB4 antibody 0618 was described before (3). Mouse monoclonal anti-parvalbumin antibody (PV235) was from Swant, monoclonal anti- calcium/calmodulin-dependent protein kinase II (CaMKII) antibody (clone 6G9) was from Chemicon, anti-β-actin antibody (NB600-503) was from Novus, goat anti-rabbit IgG conjugated with Alexa Fluor 488 (A11034) and goat anti-mouse IgG conjugated with Alexa Fluor 594 (A11005) were from Invitrogen, and horseradish peroxidase (HRP)-conjugated goat anti-rabbit antibody was from Bio-Rad.

$ErbB4^{loxP/loxP}$ and PV-Cre mice were described previously (4–6). PV-Cre;$ErbB4^{-/-}$ and control mice were housed in a room with a 12-h light/dark cycle with access to food and water ad libitum unless otherwise indicated. Experiments with animals were approved by the Institutional Animal Care and Use Committee of the Medical College of Georgia.

Electrophysiological Recordings. Slices from P42–P65 mice were prepared as described previously (2). eIPSCs were recorded in artificial cerebrospinal fluid (ACSF) containing 126 mM NaCl, 2.5 mM KCl, 1.25 mM NaH_2PO_4, 2 mM $MgSO_4$, 2 mM $CaCl_2$, 26 mM $NaHCO_3$, and 10 mM glucose. Glass pipettes were filled with the solution containing 125 mM Cs-methanesulfonate, 10 mM CsCl, 10 mM Hepes, 1 mM EGTA, 1 mM $MgCl_2$, 0.1 mM $CaCl_2$, 10 mM sodium phosphocreatine, 0.2 mM leupeptin, 4 mM Mg-ATP, 0.3 mM Na-GTP, and 5 mM QX-314 (pH 7.3, 280 mOsm) (2). Action potentials were evoked by a depolarizing 200-pA current step and recorded by whole-cell current-clamp techniques using an Axon Multiclamp 700B amplifier and pClamp 9.2 software (Molecular Devices). Glass pipettes (3–5 MΩ) were filled with the solution containing 120 mM K-gluconate, 20 mM KCl, 10 mM Hepes, 0.1 mM EGTA, 2 mM $MgCl_2$, 10 mM sodium phosphocreatine, 0.2 mM leupeptin, 4 mM Mg-ATP, and 0.3 mM Na-GTP (pH 7.3, 280 MΩ with sucrose). To minimize the effects of glutamatergic synapses, DL-AP5 (50 μM) and CNQX (20 μM) were supplemented in ACSF. In some experiments, neurons were labeled by filling recording pipettes with solution containing Oregon Green 488 biocytin (150 μM) for posthoc morphological analysis and CaMKII costaining. Only neurons with a resting potential of at least –60 mV and series resistance that fluctuated within 15% of initial values (<20 MΩ) were used for analysis. Data were filtered at 2 kHz and sampled at 10 kHz. Spontaneous firing rates were recorded extracellularly in a modified ACSF (3.5 mM KCl, 0.5 mM $MgSO_4$, 1 mM $CaCl_2$) (7) in a loose-patch cell-attached configuration. A seal of 60–200 MΩ was obtained by patching onto visually identified pyramidal neurons by using 2–3 MΩ pipettes filled with modified ACSF. Recordings were analyzed if spikes exceeded 5 mV and if the seal remained stable for >5 min.

Immunocytochemistry and Western Blot Analysis. Immunofluorescence staining and Western blot analysis were performed as previously described (2).

Behavioral Analysis. Behavioral analysis was carried out with 8- to 12-week-old mice by investigators unaware of their genotype. For the open field test, animals were placed in a chamber (27.9 × 27.9 cm) and monitored for movement by using horizontal and vertical photo beams (Med Associates). Beam breaks were converted to directionally specific movements and summated at 5-min intervals over a 30-min period. Ambulatory activity was measured as total horizontal photobeam breaks (horizontal activity), rearing was evaluated as total vertical beam breaks (vertical activity), and stereotypy was quantified in terms of repetitive breaks of a given beam with intervals of <1 s.

Working memory was evaluated by using an automated radial arm maze (Med Associates), consisting of an octagonal central platform from which eight arms radiated symmetrically. Each arm has a nose-poke response module and food pellet dispenser at the distal end. Food-restricted mice were trained to retrieve food pellets from the end of each arm. After the initial shaping, mice were allowed free access to either four arms (less difficult condition) or eight arms (more difficult condition) where all arms were baited. A mouse was first placed in the center platform and allowed to retrieve food from one arm. After it returned to the center platform, a 5-s delay followed, before all arms opened again and allowed access to all arms. The number of errors (repeated entries into a previously visited arm or omission of an arm) and the total time to retrieve all pellets were scored. Trials were terminated after all pellets were retrieved or cutoff time had elapsed (10 min for four-arm and 15 min for eight-arm tests).

PPI tests were conducted in a sound-attenuated chamber (San Diego Instruments). The motion of mice, placed in a Plexiglas tube mounted on a plastic frame, was monitored by a piezoelectric accelerometer. Before the test, mice were allowed to habituate to the chamber, to the 70-dB background white noise for 5 min, and to the prepulses (20 ms white noise at 75, 80, or 85 dB) and auditory-evoked startle stimuli (120 dB, 20 ms). In the PPI test, mice were subjected to 12 startle trials (120 dB, 20 ms) and 12 prepulse/startle trials (20 ms white noise at 75, 80, or 85 dB at 100-ms intervals and 20 ms 120-dB startle stimulus). Different trial types were presented pseudorandomly with each trial type presented 12 times, and no two consecutive trials were identical. Mouse movement was measured during 100 ms after startle stimulus onset (sampling frequency 1 kHz) for 100 ms. PPI (%) was calculated according to the formula: [100 - (startle amplitude on prepulse-pulse trials/startle amplitude on pulse alone trials) × 100]. In some experiments, diazepam (0.3 mg/mL) or vehicle was injected intraperitoneally at 10 mL/kg 30 min before the PPI test.

Statistical Analysis. Data were analyzed by paired or unpaired *t* test, one-way ANOVA followed by Dunnett's test, or repeated measures ANOVA by using SPSS software. Unless otherwise indicated, data were expressed as mean ± SEM, and statistical significance was considered when $P < 0.05$.

1. Holmes WE, et al. (1992) Identification of heregulin, a specific activator of p185erbB2. *Science* 256:1205–1210.
2. Woo RS, et al. (2007) Neuregulin-1 enhances depolarization-induced GABA release. *Neuron* 54:599–610.
3. Zhu X, Lai C, Thomas S, Burden SJ (1995) Neuregulin receptors, erbB3 and erbB4, are localized at neuromuscular synapses. *EMBO J* 14:5842–5848.
4. García-Rivello H, et al. (2005) Dilated cardiomyopathy in Erb-b4-deficient ventricular muscle. *Am J Physiol Heart Circ Physiol* 289:H1153–H1160.

5. Arber S, Ladle DR, Lin JH, Frank E, Jessell TM (2000) ETS gene Er81 controls the formation of functional connections between group Ia sensory afferents and motor neurons. *Cell* 101:485–498.
6. Hippenmeyer S, et al. (2005) A developmental switch in the response of DRG neurons to ETS transcription factor signaling. *PLoS Biol* 3:e159.
7. Maffei A, Nelson SB, Turrigiano GG (2004) Selective reconfiguration of layer 4 visual cortical circuitry by visual deprivation. *Nat Neurosci* 7:1353–1359.

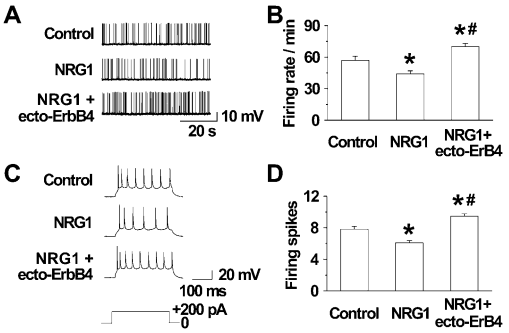

Fig. S1. NRG1 inhibition of the activity of pyramidal neurons was blocked by ecto-ErbB4. (*A*) NRG1 inhibition of spontaneous spikes was blocked by bath coapplication of 1 μg/mL ecto-ErbB4. Pyramidal neuron firings were recorded under loose patch-clamp configuration. (*B*) Quantitative analysis of data in *A* (means ± SEM; $n = 8$, $^{*}P < 0.05$ in comparison with control; $^{\#}P < 0.01$ in comparison with NRG1). (*C*) NRG1 inhibition of evoked firing frequency was blocked by bath coapplication of 1 μg/mL ecto-ErbB4. The evoked firings of PFC pyramidal neurons were recorded in a whole-cell patch-clamping configuration. (*D*) Quantitative analysis of data in *C* (means ± SEM; $n = 11$, $^{*}P < 0.05$ in comparison with control; $^{\#}P < 0.05$ in comparison with NRG1).

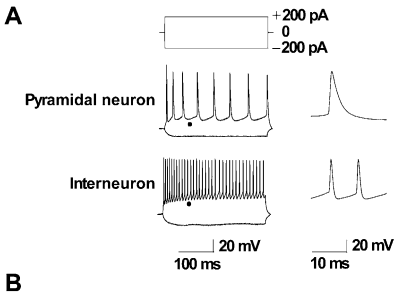

B

	Pyramidal cells	Interneurons
Spike amplitude (mV)	85.3 ± 9.4	70.1 ± 15.6
RMP (mV)	−64.3 ± 1.4	−68.7 ±1.7
Input resistance (MΩ)	163.1 ± 42.5	186.2 ± 56.3
AHP amplitude (mV)	8.7 ± 1.4	21.6 ± 1.8*
Spike width at half amplitude (ms)	0.98 ± 0.10	0.41 ± 0.07*

Fig. S2. Characterization of evoked firing of pyramidal neurons and interneuons in PFC layers II–V. (*A*) Neurons were injected with depolarizing (+200 pA) and hyperpolarizing (−200 pA) somatic currents and evoked action potentials were recorded by whole-cell patch clamping. • denotes the unit(s) expanded on the *Right*. (*B*) Distinct membrane properties of pyramidal neurons and interneurons in PFC layers II–V. Shown are means ± SEM, $n = 17$ and 12 for pyramidal cells and interneurons, respectively; $^{*}P < 0.05$ in comparison with pyramidal neurons. AHP, after hyperpolarization potential; RMP, resting membrane potential.